

Moisture Tendency Equations in a Tropical Atmosphere

C. Lopez-Carrillo* and D.J. Raymond

New Mexico Tech

*Corresponding author address: Dr. Carlos López Carrillo, Department of Physics, New Mexico
Tech, Socorro, NM 87801. E-mail clopez@kestrel.nmt.edu

Abstract

Direct diagnostic evaluation of the moisture tendency in the moisture equation is very difficult in practice because two poorly measured terms, moisture convergence and precipitation, dominate the equation. Using the near constancy in space and time of the tropical temperature profile, a variety of energy and entropy based equations have been employed to obtain indirect estimates of the moisture budget. We develop rigorous versions of the energy and entropy equations. The strengths and weakness of these two formulations are complementary, allowing us to estimate moistening and drying tendencies with high confidence when the two formulations are used together.

We apply the theory to data from TOGA-COARE. The results demonstrate how convection regulates the tropospheric humidity, drying the atmosphere when it becomes too moist, and moistening it when it becomes too dry.

1 Introduction

In the tropics several convective regimes, ranging from suppressed to deep convection, can be found (Gray (1973) , Johnson et al. (1992)). The study of these regimes is important not only for increasing our knowledge about their internal dynamics and evolution, but also for understanding the atmospheric circulations in which they are embedded. For instance, shallow convection and stratiform clouds can have a strong effect on radiative transfer; deep convective cores, on the other hand, can dominate the thermodynamic structure of the atmosphere via the latent heat release associated with their precipitation (Houze 1993).

Although determining where and when a particular kind of convection is going to occur is still an unsolved problem, several aspects of the tropical environment have been identified as critical to convection, environmental moisture being one of the most notable. For instance, modeling efforts by Neelin and Held (1987) suggest that, for a given forcing, the strength of convection depends on what they call the gross moist instability – a quantity that is closely related to the moisture in the troposphere. Their results imply that a moistened atmosphere enhances rainfall, and hence deep convection. More recent numerical efforts by Tompkins and Craig (1998) as well as Raymond and Zeng (2004) also suggest a strong dependence of precipitation upon atmospheric relative humidity. The consequences of taking this result to the limit of assuming that precipitation depends only on the atmospheric moisture were investigated by Raymond (2000). Under this assumption, he was able to extend the analysis of Neelin and Held (1987) to non-steady situations. There is

some observational evidence that atmospheric moisture, at mid-levels in particular, is correlated with the observed type of convection (Brown and Zhang, 1997), and further that mid-level moisture appears to be the primary predictor determining the strength of convection (Sherwood, 1999.) This link between mid-level moisture and convection has also been suggested by Emanuel (1994) and Raymond (1995).

There is thus a considerable amount of theoretical research, backed up by some observational results, that support the idea that the atmosphere has to be moistened in order to support deep convective regimes. The moistening process is carried out by shallower clouds which move the moisture from the boundary layer to the free troposphere. It is then generally accepted that deep convective towers act as dryers of the environment in which they are growing. Although this picture makes sense, it is difficult to observe how clouds exchange water with their environment. The major terms in the water budget equation are moisture convergence and precipitation. The small residual obtained from subtracting these terms is what determines whether the atmosphere moistens or dries. In practice, the errors associated with rain estimations are typically larger than 50%, which makes it almost observationally impossible to distinguish drying from moistening. Thus difficulties with rain estimates have undermined the study of moisture interchange. This state of affairs is what motivates our research.

In this paper, a framework is developed that enables one to identify drying or moistening of the environment without focusing on the water budget. The framework is based on the following assumption about the atmosphere: If horizontal temperature gradients are small and vertical temperature profiles do not change much with time,

then variations in the mass-weighted averages of energy and entropy depend only on variations in the amount of water in the atmosphere, and their maximum values are attained when the atmosphere becomes saturated. Thus, an increase in the average values of energy and entropy indicates moistening of the environment. In the deep tropics, horizontal and temporal gradients of temperature are very small, so this approach seems justified. Furthermore, for tropical conditions, the budgets for energy, entropy, and water can be combined to obtain equations independent of precipitation rate. We show that even when the reduced equations for energy and entropy contain certain unknown terms, they can still be used to distinguish between moistening or drying tendencies due to convective clouds in the environment.

Our approach basically consists in estimating the time rate of change of moist entropy and moist energy for a control cylinder, and then showing that when no solid precipitation reaches the surface, these tendencies can be combined with the water substance tendency in the control volume to make them independent of precipitation rate. Then, the properties of energy and entropy are invoked to argue that those terms which cannot be easily evaluated from field or model data do not prevent those equations from being useful for determining the sign of the moisture tendency inside the control volume.

The atmosphere is considered to be a multicomponent fluid whose components can flow relative to each other. This approach allows for a more accurate account of energy and entropy budgets, because it has the great advantage of regarding drag forces as internal forces. Although precipitation and cloud condensate have been included as a part of the fluid, the usual formalism used to describe inhomogeneous

mixtures of gases (de Groot and Mazur, 1962) has been followed. Note, however, that in order to treat surface fluxes cleanly, it is necessary to describe the relative motion of the fluid components with respect to dry air rather than with respect to mean air velocity. Nevertheless, the formalism remains the same. The different water phases are regarded as different components in the fluid. Furthermore, precipitation and cloud condensate are considered as different components, even when they correspond to the same water phase. The hypothetical atmosphere is therefore composed of dry air, water vapor, cloud droplets, cloud ice, liquid water precipitation, and ice precipitation. It should be pointed out that ice here represents any form of solid water. The distinction between cloud ice and precipitation ice is just that the former moves with the wind while the later falls with respect to the wind. In general, it is assumed that at any given level, dry air, water vapor, and cloud condensate (liquid and solid) all move at the same velocity, while the various forms of precipitation fall with respect to dry air. The relative concentrations among the different components in the fluid are defined in terms of mass fractions. Therefore, the value of any intensive parameter of the fluid as a whole can be written as the mass-weighted average over all the components of the fluid.

This paper is arranged as follows: budget equations for water substance, energy, and entropy, appropriate to the atmosphere, are presented in section 2; the moistening and drying equations are developed in section 3; an application of the proposed theory is presented in section 4; a summary and discussion is given in section 5; explicit forms for the energy and entropy that consistently handle all water phases are presented in the appendix.

2 Budget equations

2.1 Water substance

The mass budget in an Eulerian control volume, \mathcal{V} , for the j th component in our fluid can be written as

$$\frac{d}{dt} \int_{\mathcal{V}} \rho_j d\mathcal{V} + \oint_{\mathbf{A}} \rho_j \mathbf{v}_j \cdot \hat{\mathbf{n}} d\mathbf{A} = \mathcal{S}_j \quad (1)$$

where \mathbf{A} is the boundary of \mathcal{V} , $\hat{\mathbf{n}}$ is the normal vector pointing outwards from the boundary surface \mathbf{A} , and ρ_j, \mathbf{v}_j are the density and mean velocity of the j th component in the fluid. The quantity \mathcal{S}_j is the mass source per unit volume for this component. For instance, it is equal to zero for dry air. On the other hand, in the case of water vapor, it could represent the conversion rate between water vapor and condensate. In general, estimating rates of conversion among different phases of water is a very difficult task. Fortunately, because water is just transformed among the different phases, the net source for total water inside any control volume is zero. Therefore, the budget of total water substance in an arbitrary fixed control volume is reduced to the balance between the increase in total mass of water inside the volume and the inflow of the different water components. Writing the velocities for the water components with respect to the velocity of dry air, \mathbf{v}_d , results in the following budget equation for water substance:

$$\frac{d}{dt} \int_{\mathcal{V}} \rho_w d\mathcal{V} = - \oint_{\mathbf{A}} (\rho_w \mathbf{v}_d + \mathbf{D}_w) \cdot \hat{\mathbf{n}} d\mathbf{A} \quad (2)$$

where $\rho_w = \sum \rho_j$, and $\mathbf{D}_w = \sum \rho_j (\mathbf{v}_j - \mathbf{v}_d)$, the sums being over the various water substance components. This equation plays a very important role in the derivation

of the final energy and entropy budget equations.

2.2 Energy

The total energy per unit mass, e , of the fluid is defined as the mass-weighted average of the specific energies of all the fluid's components. The total energy for each of the components is in turn the sum of internal, kinetic, and potential energies.

A succinct form of the energy budget equation can be obtained in terms of the Bernoulli function. For fluids in general, the Bernoulli function is defined as the sum of kinetic and potential energies per unit mass plus the specific enthalpy of the system. Hence, the Bernoulli function for the j th component of the fluid is written as $b_j = e_j + P_j/\rho_j$, where e_j , P_j , and ρ_j are the total energy per unit mass, partial pressure, and density. In the range of atmospheric conditions there is essentially no difference between enthalpy and internal energy for ice and liquid, and the Bernoulli function for a condensate is equal to the total energy of condensate per unit mass.

Since the gaseous components in the atmosphere behave like ideal gases, their Bernoulli functions can be written as $b_j = e_j + R_j T_j$ where T_j and $R_j = R_g/\mathcal{M}_j$ are the absolute temperature and gas constant, defined as the universal gas constant divided by the molecular weight of the gas. This expression can also be used for condensed substances by setting their gas constants to zero. Therefore, the Bernoulli function of the j th component in our system can in general be written as $b_j = e_j + R_j T_j$, where R_j is the associated gas constant (set to zero for condensed matter). As with e , the total Bernoulli function is defined as the mass-weighted aver-

age of the individual Bernoulli functions in the mix, resulting in $b = e + P/\rho$, where e is the total energy, P is the fluid pressure and ρ is the total density. In terms b , the energy budget equation can be written as

$$\frac{d}{dt} \int_V \rho e \, dV + \oint_A (\rho b \mathbf{v}_d + \mathbf{J}_c + \mathbf{J}_w + \mathbf{D}_b - \overleftrightarrow{\nu} \cdot \mathbf{v}) \cdot \hat{\mathbf{n}} \, dA = \mathcal{R}_e \quad (3)$$

where

$$\mathcal{R}_e = - \int_V \nabla \cdot \mathbf{J}_R \, dV \quad (4)$$

is the external radiative source of energy. In deriving this equation, the velocities of the individual components in the mass transport contributing terms are written with respect to the dry air velocity, \mathbf{v}_d , which gives rise to the Bernoulli flux relative to dry air:

$$\mathbf{D}_b = \sum_j \rho_j b_j (\mathbf{v}_j - \mathbf{v}_d) \quad (5)$$

where b_j is the Bernoulli function of the j th component. Note however that the mean velocity of the fluid, \mathbf{v} , is kept in the term associated with the surface stresses, $\overleftrightarrow{\nu} \cdot \mathbf{v}$. Contributions to the budget from conduction and radiation are written in terms of the radiative, \mathbf{J}_R , and conductive, \mathbf{J}_c , heat fluxes. Since radiation energy is always present in the atmosphere, and some of it may travel well beyond the surface of the control volume before interacting with the system's matter, or may not interact at all, it is conceptually advantageous to exclude the radiation field from our system. That is why the radiative contribution is written as an external source, even though mathematically, it could be written as a flux of energy passing through the surface of V . Another assumption made in deriving equation (3) is that all body forces acting on our fluid are conservative, and their effects are accounted for in the potential energy

term. One of the advantages of using total energy is that the effects of internal forces (like drag between condensate and gas) are implicitly taken into account. This is so because all they do is to redistribute energy among its different forms. Hence they do not change the total energy. On the other hand, surface forces acting over the periphery of our volume, including dissipative and non-dissipative effects, could change the energy inside V . Therefore, they have to be accounted for explicitly in the energy budget. Their effect is represented using the Newtonian stress tensor, $\overleftrightarrow{\nu}$. It should be pointed out that in order to exclude variations associated with gravity wave transport phenomena from the velocity fields and thermodynamic pressure, all surface forces due to waves moving in or out of V are excluded from $\overleftrightarrow{\nu}$. Account for wave transport is made explicitly via the wave-energy flux vector, \mathbf{J}_w .

2.3 Entropy

The derivation of the entropy budget makes use of the common assumption that the atmosphere is in a state of local thermodynamic equilibrium. The total entropy per unit mass of the system, s , is defined as the mass-weighted average of the specific entropies of the fluid's components. In order to obtain an appropriate form of the entropy budget equation, the contributions to the entropy tendency, except those due to radiative heating, were separated in two categories: fluxes of entropy due to interactions between the system and its environment, which can be directed in or out of the system, and sources of entropy due to irreversible interactions within the system. Since the sources just defined only increase the entropy inside the system,

their combined contribution is referred to, in a generic way, as “the irreversible generation of entropy” and will be denoted by σ . This separation is extremely useful, for it allows us to reach our goal without detailed knowledge of entropy sources. Entropy fluxes, on the other hand, must be carefully accounted for. Writing the velocities of the fluid’s components with respect to the dry air velocity leads to the following form of the entropy flux due to mass transport

$$\mathbf{J}_s = \rho s \mathbf{v}_d + \mathbf{D}_s \quad (6)$$

where \mathbf{v}_d is the dry air velocity, ρ and s are the total density and entropy of the system, respectively, and

$$\mathbf{D}_s = \sum_j \rho_j s_j (\mathbf{v}_j - \mathbf{v}_d) \quad (7)$$

is the entropy flux relative to dry air. Note that associated with this flux there is a source of entropy whose value is lumped into σ . The convergence of conductive heat flux produces an entropy tendency given by

$$-\frac{1}{T} \nabla \cdot \mathbf{J}_c \quad (8)$$

where T is the absolute temperature and \mathbf{J}_c is the conductive heat flux. This can be formally separated into an entropy flux convergence

$$F_{cs} = -\nabla \cdot \left(\frac{\mathbf{J}_c}{T} \right) \quad (9)$$

and an irreversible entropy source

$$S_{cs} = -\frac{1}{T^2} \mathbf{J}_c \cdot \nabla T \quad (10)$$

This source, which always increases the value of the entropy, is also incorporated into σ . Similarly, the change in entropy due to radiative heating is given by

$$-\frac{1}{T} \nabla \cdot \mathbf{J}_R \quad (11)$$

where \mathbf{J}_R is now the radiative heat flux. However in this case, the separation between flux and irreversible source is only clear in the limit of diffusive radiation (Mihalas and Mihalas, 1984). The fundamental difference is that conductive heat fluxes are set up by the local gradient in temperature, while radiative heat fluxes need not be related to local temperature gradients. These complexities force us to treat radiation as an external source of entropy which could increase or decrease the entropy of the system. Nevertheless, this is consistent with the idea of considering the radiation field as outside of our system.

Collecting all contributions, the entropy budget equation may be written as

$$\frac{d}{dt} \int_V \rho s \, dV + \oint_A \left[\rho s \mathbf{v}_d + \mathbf{D}_s + \frac{1}{T} \mathbf{J}_c \right] \cdot \hat{\mathbf{n}} \, dA = \mathcal{R}_s + \mathcal{G} \quad (12)$$

where

$$\mathcal{R}_s = - \int_V \frac{1}{T} \nabla \cdot \mathbf{J}_R \, dV \quad (13)$$

is the external radiative source of entropy and

$$\mathcal{G} = \int_V \rho \sigma \, dV \quad (14)$$

is the source of entropy due to irreversible generation.

3 Moistening and drying tendency equations

As mentioned in the introduction, a major drawback in using water budgets to study moistening or drying of the environment is the great uncertainty in precipitation measurements. Here we develop equations that can be used to identify drying or moistening which do not depend on precipitation. The starting point is the estimation of the time rate of change for water substance, energy, and entropy in a control cylinder that extends from the surface to an upper boundary extending above all convection. The lateral boundary of this cylinder has to be large enough to enclose the whole convective system.

In order to make the estimations possible, some approximations are in order: The horizontal velocity of cloud condensate will be regarded as equal to the horizontal mean velocity of the fluid; no flux of matter is allowed at the upper boundary; the temperatures are assumed to be uniform at the lower and upper boundaries of the control volume; and the conductive heat flux is neglected everywhere except at the lower boundary of the control volume. Under these assumptions, the time rate of change for the average value of water substance in our fixed control volume can be written as

$$\frac{d\overline{\rho_w}}{dt} = - \frac{1}{A H} \left\{ \int_{\text{lat}} \rho_w \mathbf{v}_d \cdot \hat{\mathbf{n}}_l \, da + \int_{\text{bot}} \mathbf{D}_w \cdot \hat{\mathbf{k}} \, da \right\} \quad (15)$$

where H and A are the height and horizontal area of the control cylinder, respectively. Since at the bottom surface the fluxes are due only to evaporation and precipitation, and the vertical component of the mean dry air velocity is zero at that surface, the

flux of water substance relative to dry air at the bottom surface can be simplified to:

$$\mathbf{D}_w \cdot \hat{\mathbf{k}} = (\rho_v \mathbf{v}_v + \rho_{lp} \mathbf{v}_{lp} + \rho_{ip} \mathbf{v}_{ip}) \cdot \hat{\mathbf{k}} \quad (16)$$

where the subindexes v , lp , and ip refer to vapor, liquid precipitation and ice precipitation, respectively. This simplification is the reason for defining relative velocities with respect to dry air. The flux of water vapor at the surface, $\rho_v \mathbf{v}_v \cdot \hat{\mathbf{k}}$, is by definition, just the evaporation rate \mathcal{E} , and the vertical flux of liquid and ice ($\rho_{lp} \mathbf{v}_{lp} \cdot \hat{\mathbf{k}}$, $\rho_{ip} \mathbf{v}_{ip} \cdot \hat{\mathbf{k}}$) are just the precipitation rates of liquid and ice, \mathcal{P}_l , \mathcal{P}_i , respectively. Hence, the tendency equation for the average value of water substance inside the control cylinder can be written as:

$$\frac{d\overline{\rho_w}}{dt} = -\frac{1}{AH} \left\{ \int_{\text{lat}} \rho_w \mathbf{v}_d \cdot \hat{\mathbf{n}}_l \, da + \int_{\text{bot}} (-\mathcal{E} + \mathcal{P}_l + \mathcal{P}_i) \, da \right\} \quad (17)$$

The minus in front of \mathcal{E} is due to the fact that evaporation is defined as going into the atmosphere and the normal at the surface is pointing downwards.

In a very similar way and under the same assumptions, a tendency equation for the average of the total energy inside the control cylinder can be derived:

$$\begin{aligned} \frac{d\overline{\rho e}}{dt} = & -\frac{1}{AH} \left\{ \int_{\text{lat}} \rho b \mathbf{v}_d \cdot \hat{\mathbf{n}}_l \, da + \right. \\ & \left. + \int_{\text{bot}} \left[\mathbf{J}_c \cdot (-\hat{\mathbf{k}}) - \mathcal{E} b_{v,b} + \mathcal{P}_l b_{lp,b} + \mathcal{P}_i b_{ip,b} \right] \, da \right\} \\ & + \overline{\mathcal{L}} + \overline{\mathcal{W}} + \overline{\mathcal{R}}_e \end{aligned} \quad (18)$$

where $b_{v,b}$, $b_{lp,b}$, and $b_{ip,b}$ are the Bernoulli functions of vapor, liquid precipitation and ice precipitation at the bottom surface, respectively;

$$\overline{\mathcal{L}} = \frac{1}{AH} \oint_{\mathbf{A}} \overleftrightarrow{\mathbf{v}} \cdot \mathbf{v} \cdot \hat{\mathbf{n}} \, d\mathbf{A} \quad (19)$$

is the total energy dissipated by frictional stress at the surface of the control cylinder,

$$\overline{W} = - \frac{1}{A H} \oint_A \mathbf{J}_w \cdot \hat{\mathbf{n}} \, dA \quad (20)$$

is the total energy transfer associated with wave phenomena; and

$$\overline{\mathcal{R}}_e = - \frac{1}{A H} \int_V \nabla \cdot \mathbf{J}_R \, dV \quad (21)$$

is the average rate of change of energy due to radiation.

The tendency equation for the average entropy is given by:

$$\begin{aligned} \frac{d\overline{\rho s}}{dt} = & - \frac{1}{A H} \left\{ \int_{\text{lat}} \rho \, da \, s \mathbf{v}_d \cdot \hat{\mathbf{n}}_l \, da \right. \\ & \left. + \int_{\text{bot}} \left[\frac{\mathbf{J}_c}{T_s} \cdot (-\hat{\mathbf{k}}) - \mathcal{E}_{s_{v,b}} + \mathcal{P}_l s_{lp,b} + \mathcal{P}_i s_{ip,b} \right] da \right\} + \overline{\mathcal{R}}_s + \overline{\mathcal{G}} \quad (22) \end{aligned}$$

where $s_{v,b}$, $s_{lp,b}$, $s_{ip,b}$ are the entropy of vapor, liquid precipitation and ice precipitation at the bottom surface, respectively, and T_s is the surface temperature;

$$\overline{\mathcal{R}}_s = - \frac{1}{A H} \int_V \frac{1}{T} \nabla \cdot \mathbf{J}_R \, dV \quad (23)$$

is the average change in entropy due to radiation; and

$$\overline{\mathcal{G}} = \frac{1}{A H} \int_V \rho \sigma \, dV \quad (24)$$

is the average irreversible generation of entropy inside the control cylinder.

The tendency equations for energy and entropy may be combined with that for water substance to eliminate precipitation rates. However, both ice and liquid water precipitation cannot be eliminated simultaneously. Hence, it has to be assumed that one of them is zero. In the deep tropics, it is reasonable to assume that no ice precipitation reaches the surface. Another required assumption is that temperature

and pressure are constant on the bottom surface and that the kinetic energy is much smaller than the internal energy there. This means that the total energy and entropy can be considered constant at the bottom surface of the control cylinder. With these additional assumptions, multiplying the tendency equation of water substance by $b_{l,b}$ and subtracting the result from the energy tendency equation results in

$$\begin{aligned} \frac{d\overline{\rho(e - q_w e_{lp,b})}}{dt} &= -\frac{1}{AH} \left\{ \int_{\text{lat}} \rho (b - q_w b_{lp,b}) \mathbf{v}_d \cdot \hat{\mathbf{n}}_l \, da + \right. \\ &\quad \left. + \int_{\text{bot}} [\mathbf{J}_c \cdot (-\hat{\mathbf{k}}) - \mathcal{E}(b_{v,b} - b_{lp,b})] \, da \right\} \\ &\quad + \overline{\mathcal{L}} + \overline{\mathcal{W}} + \overline{\mathcal{R}}_e \end{aligned} \quad (25)$$

where q_w is the mass fraction of total water. The fact that the total energy and Bernoulli function are the same for condensed matter has been used.

Defining the reduced energy and Bernoulli functions as

$$\tilde{e} = e - q_w e_{lp,b} \quad (26)$$

$$\tilde{b} = b - q_w b_{lp,b} \quad (27)$$

results in a new tendency equation:

$$\begin{aligned} \frac{d\overline{\rho\tilde{e}}}{dt} &= -\frac{1}{AH} \left\{ \int_{\text{lat}} \rho \tilde{b} \mathbf{v}_d \cdot \hat{\mathbf{n}}_l \, da + \right. \\ &\quad \left. - \int_{\text{bot}} [\mathbf{J}_c \cdot \hat{\mathbf{k}} + \mathcal{E}(b_{v,b} - b_{lp,b})] \, da \right\} + \overline{\mathcal{L}} + \overline{\mathcal{W}} + \overline{\mathcal{R}}_e \end{aligned} \quad (28)$$

Two things are notable about this equation: 1) It does not depend on precipitation. 2) The source terms are the same as those of the tendency equation of total energy.

Similarly, multiplying the tendency equation for total water by $s_{lp,b}$, and subtracting the result from the tendency equation of entropy (22), leads to

$$\frac{d\overline{\rho\tilde{s}}}{dt} = -\frac{1}{AH} \left\{ \int_{\text{lat}} \rho \tilde{s} \mathbf{v}_d \cdot \hat{\mathbf{n}}_l \, da \right.$$

$$- \int_{\text{bot}} \left[\frac{\mathbf{J}_c}{T_s} \cdot \hat{\mathbf{k}} + \mathcal{E}(s_{v,b} - s_{lp,b}) \right] da \Big\} + \overline{\mathcal{R}}_s + \overline{\mathcal{G}} \quad (29)$$

where the reduced entropy has been defined as

$$\tilde{s} = s - q_w s_{lp,b} \quad (30)$$

The tendency equation for this new variable does not contain precipitation and its sources are the same as those for the entropy tendency equation.

Although the reduced equations do not contain precipitation, they still have the unknown sources of original energy and entropy budget equations. The following argument shows that only fluxes and radiation sources are required to determine whether moistening or drying is occurring in an atmospheric column.

Let us rewrite equations (28) and (29) as follows:

$$\frac{d\overline{\rho \tilde{e}}}{dt} = I_e + \overline{\mathcal{L}} + \overline{\mathcal{W}} \quad (31)$$

$$\frac{d\overline{\rho \tilde{s}}}{dt} = I_s + \overline{\mathcal{G}} \quad (32)$$

where

$$I_e = -\frac{1}{AH} \left\{ \int_{\text{lat}} \rho \tilde{b} \mathbf{v}_d \cdot \hat{\mathbf{n}}_l da + \int_{\text{bot}} \left[\mathbf{J}_c \cdot \hat{\mathbf{k}} + \mathcal{E}(b_{v,b} - b_{lp,b}) \right] da \right\} + \overline{\mathcal{R}}_e \quad (33)$$

and

$$I_s = -\frac{1}{AH} \left\{ \int_{\text{lat}} \rho \tilde{s} \mathbf{v}_d \cdot \hat{\mathbf{n}}_l da - \int_{\text{bot}} \left[\frac{\mathbf{J}_c}{T_s} \cdot \hat{\mathbf{k}} + \mathcal{E}(s_{v,b} - s_{lp,b}) \right] da \right\} + \overline{\mathcal{R}}_s \quad (34)$$

are the flux and radiation terms in (28) and (29), respectively.

Since $\overline{\mathcal{G}}$ is the internal generation of entropy for a system that is not in equilibrium, it must be positive. On the other hand $\overline{\mathcal{L}}$ is negative, since it represents viscous forces acting on the boundaries of the control cylinder. The net wave energy source, $\overline{\mathcal{W}}$, is also negative under the assumption that the dynamical response of a less active environment consumes energy from the convection. Hence, a situation where I_e is negative implies that $d\overline{\rho\tilde{e}}/dt$ is also negative. On the contrary, positive values of I_e leave the sign of $d\overline{\rho\tilde{e}}/dt$ undetermined. Positive values of I_s , on the other hand, imply that $d\overline{\rho\tilde{s}}/dt$ is also positive, while for negative values of I_s the reduced entropy equation is not conclusive.

Thus even when $\overline{\mathcal{L}}$ and $\overline{\mathcal{W}}$ are unknown, the reduced energy equation can still be used to tell whether drying is occurring in the control cylinder, but it cannot give a conclusive answer about moistening situations. We call this equation the “the drying tendency equation”. Likewise when $\overline{\mathcal{G}}$ is unknown, the reduced entropy equation is still able to tell whether moistening is taking place. Therefore, we call it, “the moistening tendency equation”.

4 Convection and column moisture

In this section, we present a simple application of the proposed theory. The problem we want to examine is the contribution of lateral fluxes to a column’s moisture.

The application deals with mesoscale systems observed over the western Pacific warm pool. This is a region characterized by sea surface temperatures that exceed 28°C, and extends approximately from 10°S to 10°N and from 140°E to 170°E. The

observations took place from November 1, 1992 to February 28, 1993 during the intensive observation period (IOP) of TOGA-COARE (Tropical Ocean Global Atmosphere - Coupled Ocean Atmosphere Response Experiment; Webster and Lukas, 1992).

We take advantage of the myriad of meteorological observations that were taken over the IFA (Intensive Flux Array) and explore two different approaches to the estimation of lateral fluxes. This allows us to get a sense for the robustness of the conclusions resulting from the application of different data sets to the lateral entrainment problem.

4.1 Lateral fluxes from sounding array

For the first method, we employ the soundings deployed around the IFA of TOGA-COARE (see figure 1).

Satellite observations are available from the Japanese satellite GMS-4 (Flament and Bernstein, 1993) every hour during the IOP with very few gaps. The satellite infrared temperature averaged over the IFA is used as a surrogate for convection in the column. The resulting time series is presented in the upper panel of figure 2.

Lateral fluxes are estimated using the information available from radiosondes launched every six hours at the corners of the IFA. Hence, in this method the wind velocities and thermodynamic quantities around the control cylinder come from interpolating the observations made at the sounding sites. In our case, we use simple linear interpolation between soundings launched from Kapingamarangi, Kavieng, and the ships *Xiangyanghong 5* and *Shiyan 3*. The fluxes are calculated from Feb 3 to

Feb 13 (days 95 to 105 of the IOP) because during this period we have soundings from all four corner stations.

We start by processing each sounding in the following way: From sounding measurements (pressure, environmental temperature, dewpoint temperature and horizontal winds), we derive the reduced entropy and Bernoulli functions using the formulas given in the appendix. Then, we interpolate all quantities to a regular vertical grid with 100 m grid steps.

In order to obtain an accurate estimate of lateral mass transport, we correct the horizontal velocities of the soundings by demanding mass continuity in the column. The corrections are calculated from soundings taken at the corners of the IFA launched at the same nominal time. It is assumed that horizontal velocities vary linearly between sounding sites and that mass density varies only in the vertical. Implicit in the calculations is the assumption of no mass fluxes either through top or bottom lids of the column. This assumption is not completely accurate due to evaporation, precipitation and surface pressure changes. However, for the purposes of mass balance these are very small corrections. The more demanding assumption is the linear model for the velocities. The velocities are corrected by adding to them a constant-magnitude vector, \mathbf{C} , which points in the same direction as the outward normal, $\hat{\mathbf{n}}$, to the perimeter and whose magnitude is such that the resulting velocities satisfy mass continuity. Given the above assumptions the velocity correction is given by

$$|\mathbf{C}| = - \frac{A}{PM} \int_0^{top} \oint_P \rho(z) \mathbf{u}(l) \cdot \hat{\mathbf{n}} dl dz \quad (35)$$

where ρ, P, A , and M , are the density, perimeter, horizontal area, and mass, of the IFA column, respectively.

In order to estimate the lateral import per unit volume of the reduced Bernoulli function, a linear variation of this function between stations is also assumed, and the lateral import per unit volume is given by the following bi-linear model

$$I_{\tilde{b}} = - \frac{1}{AH} \int_0^H \oint_P \rho \tilde{b}(l) \mathbf{u}(l) \cdot \hat{\mathbf{n}} \, dl \, dz \quad (36)$$

where P and A are the perimeter and the horizontal area of the IFA column, and H is the height of the column (here taken as 20 km). The results for the reduced Bernoulli function are presented in the middle panel of figure 2. A similar procedure is taken for the reduced entropy and the results are presented in the lower panel of figure 2.

Examination of the three panels of figure 2 reveals large diurnal variations in the lateral fluxes. Averaging over these variations, the lateral fluxes tend to moisten the IFA column when the spatially averaged infrared temperature is dominated by shallow clouds (days 95 to 101). On the other hand, when the average infrared temperature is dominated by deeper clouds (days 101 to 105), the lateral fluxes tend to dry the IFA column.

4.2 Lateral fluxes from radar data

For this method, we determine the lateral mass flux of a convective system from Doppler radar data and the thermodynamic structure of the atmosphere is obtained from a sounding launched close to the system. This approach has the advantage of yielding more accurate estimates of mass flux from a system than is available

from the sounding array. However, the use of a single sounding to represent the thermodynamics of the environment where the system develops is certainly an oversimplification.

Estimates of the lateral fluxes are based on the argument that gravity waves propagate faster than air parcels. Hence, the divergence field generated by the convection is felt at the border of a control cylinder (in the clear region surrounding the system) before air parcels from the system reach that border. Consequently, we assume that the air being exported from the system is coming from the clear air region surrounding the system. Further assuming horizontal homogeneity in this region enables us to use a single sounding to characterize the thermodynamics of the troposphere around the system. Hence, the lateral import of thermodynamic quantities per unit volume is given by

$$I = -\frac{A_C}{A H} \int_0^H \chi_e(z) F(z) dz \quad (37)$$

where H and A are the height and horizontal area of the control cylinder, A_C is the radar-sampled area, $\chi_e(z)$ is the sounding profile of any intensive thermodynamic variable, and

$$F(z) = \frac{1}{A_C} \int_{A_C} \nabla_h \cdot (\rho \mathbf{v}_h) da \quad (38)$$

is the average mass divergence from the convection. Note, that equation (37) assumes that other sources of divergence are small compared to divergence due to the convection.

For our analysis, we use the data collected by the X-band Doppler radars mounted on the tails of the WP3-42 and WP3-43 NOAA aircraft. The mass fluxes are derived

using the technique of Raymond et. al. (1997) with the translation velocity of the systems taken from Kingsmill and Houze (1999). The selected radar missions for this analysis as well as the sounding chosen to characterize their surrounding environment are listed in table 1. This table also shows the time interval for which the radar data are analyzed in each mission. The Cartesian grid to which Doppler velocities are interpolated is large enough to accommodate all data in the selected time interval. The grid step in the vertical is 1 km and 5 km in the horizontal. The sounding data are processed as in section 4.1, but the vertical interpolation is to a 1 km grid.

The horizontal mass divergence profiles derived from the interpolated velocities are shown in figure 3. They are divided into two groups according to the depth of their inflow layer. Combining these mass fluxes with the thermodynamic profiles according to equation (37) yields an estimate for the net import of the thermodynamic quantities. The results for the reduced entropy and Bernoulli functions for ten case studies are summarized in table 2.

Although we have accomplished the purpose of the exercise, namely identifying which systems dry and which moisten the environment, the fact that the case studies divided themselves into two categories suggests an inquiry about the humidity of the environment in which the systems were observed. For each system, the humidity of the environment is estimated by calculating the saturation deficit averaged over a 9 km layer (1-10 km). These values are listed in table 2. The sample mean of the saturation deficit for systems characterized by a shallow inflow layer is $\overline{\delta q_l} = 2.86 \text{ g kg}^{-1}$, while for systems with deep inflow layers is $\overline{\delta q_a} = 1.94 \text{ g kg}^{-1}$. The difference between these sample means is significant to the 99% confidence level using the non-parametric

Mann-Whitney U-test. Therefore, the environments in which the systems grow can also be divided into two categories which we, subjectively, call dry and moist.

The results of this section are summarized in figure 4 which shows the relationship between import of the reduced functions and saturation deficit of the environment. This plot strongly suggests that when the environment is humid, the convection tends to dry the environment. On the other hand when the environment is dry, convection tend to moisten it. Hence, it is reasonable to conclude that convection acts to regulate the moisture of the tropical environment.

5 Summary and discussion

In this work, we have derived rigorously equations for the budgets of water, energy and entropy. We have shown that when no solid precipitation hits the ground, these equations can be combined to eliminate the unmeasurable precipitation terms in the energy and entropy equations altogether. The analysis of the reduced energy equation shows that sources related to dissipation and wave transport phenomena are not required to infer a drying tendency in the environment, and that the reduced entropy equation does not require the term that represents the irreversible generation of entropy to infer a moistening tendency.

In section 4, an application of the proposed theory is presented. Though simple, that application is far from trivial. It provides insight on how lateral energy and entropy fluxes, presumably due to the action of convection, help govern the humidity of the environment. In particular, these fluxes tend to drive the humidity toward

some equilibrium value, moistening the atmosphere when it is too dry, and drying it when it is too moist. These results rest on strong assumptions about the spatial variability of thermodynamic variables. Nevertheless, the conclusion about the role of convection in regulating the environmental moisture seems to be robust under different sets of assumptions.

It is also worth noting that, although the developed theory firmly establishes which thermodynamic variable to use to decide whether drying or moistening is occurring, the observational results strongly suggest that one can obtain the same conclusions regardless of which thermodynamic variable is used.

Acknowledgments. This work was supported by the National Science Foundation Grants ATM-9616290 and ATM-0082612.

A Appendix

In this appendix, explicit forms for the energy and entropy that consistently handle all water phases are presented. It is assumed that the internal energy and the entropy per unit mass depend only on temperature, pressure and moisture. The system, i.e. the hypothetical atmosphere, consists of dry air, water vapor, cloud liquid water, cloud ice, precipitating liquid water, and precipitating ice. The mass fractions for these components are represented by q_d , q_v , q_{cl} , q_{ci} , q_{lp} , and q_{ip} , respectively. The values of the constants that appear in the equations that follow can be found elsewhere (see for instance Emanuel, 1994) .

Internal energy

The internal energy per unit mass of the j th component of a multicomponent fluid can be defined as

$$u_j = c_{vj}(T_j - T_r) + u_{rj} \quad (39)$$

where u_{rj} , c_{vj} , and T_j are the internal energy at some arbitrary reference point, heat capacity at constant volume, and absolute temperature, respectively. The absolute temperature at the reference point is denoted by T_r . This definition is quite general and can be used with gases as well as liquids and solids. Note, however, that for condensed matter in the atmospheric range of pressures, there is almost no difference between heat capacities at constant pressure and constant volume.

It is important to realize that while the internal energies of the different water phases are independent of the internal energy for dry air, they are not independent of each other. This is because there are well defined energy gaps that separate the different phases of the water substance. That is, the energy released at constant pressure during a transformation from a less to a more ordered phase is, by definition, the latent heat of the transition. Typically this is written in terms of enthalpies

$$h_v - h_l = L_v(T) \quad (40)$$

$$h_v - h_i = L_s(T) \quad (41)$$

$$h_l - h_i = L_f(T) \quad (42)$$

where $L_v(T)$, $L_f(T)$, and $L_s(T)$ are, respectively, the latent heats of evaporation, fusion, and sublimation at the temperature at which the transitions occurs. The

enthalpy of the j th component in the mix can be defined as

$$h_j = u_j + R_j T_j \quad (43)$$

where u_j , T_j are the internal energy and temperature of the j th component. Since there is essentially no difference between the enthalpy and internal energy for the condensed phases, the gas constant, R_j , is set to zero in those cases. Otherwise it is given by $R_j = R_g/\mathcal{M}_j$, where R_g is the universal gas constant and \mathcal{M}_j is the molecular mass of the gas.

Although equations (40 – 42) are defined for different temperature ranges, all ranges contain the triple point of water. For this reason, we choose the triple point of water as the reference point for the internal energies of the water phases. Hence at this reference point, equations (40 – 43) lead to the following relationships among the reference constants.

$$u_{rv} = u_{rl} + L_v(T_r) - R_v T_r \quad (44)$$

$$u_{rv} = u_{ri} + L_s(T_r) - R_v T_r \quad (45)$$

$$u_{rl} = u_{ri} + L_f(T_r) \quad (46)$$

where T_r is the temperature at the triple point of water, and it has been assumed that water vapor behaves like an ideal gas with gas constant, R_v . Since only two of these relationships are independent, one of the three reference constants must be chosen arbitrarily.

The total internal energy per unit mass is simply the mass weighted average of

the internal energies of the subsystems

$$u = \sum_j q_j u_j \quad (47)$$

where u_j is given by equation (39) and q_j is the corresponding mass fraction. Since the reference constants are subject to the constraints (44–46), an expression for the total energy can then be written as

$$u = q_v [L_v(T_r) - R_v T_r] - (q_{ci} + q_{ip}) L_f(T_r) + \sum_j q_j c_{vj} (T_j - T_r) \quad (48)$$

where the reference values of the dry air and liquid water energies have been set to zero. The summation extends over all components of the atmosphere, which may have different temperatures, T_j .

Potential energy

Assuming that the only potential energy in the system is that due to the geopotential, the potential energy per unit mass of the j th component is given by the geopotential

$$\phi_j = g z \quad (49)$$

where g is the acceleration of the gravity and z is the altitude above sea level. Therefore, the total potential energy per unit mass reduces to

$$\phi = g z \quad (50)$$

Kinetic energy

The kinetic energy per unit mass of the system is defined as

$$K = \sum_j q_j k_j \quad (51)$$

The kinetic energy per unit mass of the j th component is simply $k_j = \frac{1}{2} \mathbf{v}_j \cdot \mathbf{v}_j$, where \mathbf{v}_j is the flow velocity of the j th component.

Total energy

The total energy per unit mass for the j th component is simply the sum of the internal, potential, and kinetic energies associated with that component. In turn, the total energy per unit mass for the system has been defined as the mass-weighted average of the total energies of the individual components in the fluid.

$$e = u + gz + \sum_j q_j k_j \quad (52)$$

where u is given by equation (48). Inside a convective system, the kinetic energy typically can not be exactly estimated. But away from the system, the horizontal velocities are much larger than the vertical component, and sounding values could be used for the estimation. It turns out, however, that this contribution to the total energy is so much smaller than the internal and potential energies that, to a good approximation, it can be ignored in most cases.

Bernoulli function

The Bernoulli function per unit mass of the j th component of the system is simply the enthalpy plus the kinetic and potential energies of the component. This can be written (see section 2.2) as

$$b_j = e_j + R_j T_j \quad (53)$$

where e_j , T_j , R_j are the total energy, absolute temperature, and gas constant of the j th component. Recalling that the gas constant for the condensed phases is zero and that the gaseous components share the same temperature, T , the expression for the total Bernoulli function can be written as

$$b = e + T(q_d R_d + q_v R_v) \quad (54)$$

where e is given by equation (52).

Entropy

The entropy per unit mass of the j th component in a multicomponent fluid is defined as

$$s_j = c_{pj} \ln(T_j/T_r) - R_j \ln(P_j/P_r) + s_{rj} \quad (55)$$

where s_{rj} , c_{pj} , T_j , and P_j are the entropy at the arbitrary reference point, heat capacity at constant pressure, absolute temperature, and pressure for this component, respectively. The absolute temperature and pressure at the reference point are T_r and P_r , respectively. The gas constant, R_j , is set to zero for all condensed phases.

As with the energy, the entropies for the water phases are not independent. In this case, however, it is because the temperature, pressure, and the chemical potentials of the coexisting phases must be equal in thermodynamic equilibrium. The chemical potential of the j th component is defined as

$$\mu_j = h_j - s_j T_j \quad (56)$$

where h_j and s_j are the enthalpy and entropy per unit mass, respectively, and T_j is the absolute temperature.

Using the definition for latent heat of vaporization, equation (40), the equilibrium condition between vapor and liquid water at temperature T can be written as

$$s_v^*(T) = s_l(T) + \frac{L_v(T)}{T} \quad (57)$$

where $s_v^*(T)$ is the entropy of water vapor at saturation. It follows from (55) that

$$s_v(T, P_v) = s_v^*(T) - R_v \ln[P_v/P_v^*(T)] \quad (58)$$

where $P_v^*(T)$ is the saturation vapor pressure at temperature T . The equilibrium condition gives a general relationship between the entropy of water vapor and liquid water:

$$s_v(T, P_v) = s_l(T) + \frac{L_v(T)}{T} - R_v \ln(H_l) \quad (59)$$

where $H_l = P_v/P_v^*$ is the relative humidity with respect to liquid, and the temperatures are in the domain of the vapor-liquid equilibrium curve. Similarly, from the equilibrium condition between ice and vapor, it follows that

$$s_v(T, P_v) = s_i(T) + \frac{L_s(T)}{T} - R_v \ln(H_i) \quad (60)$$

where H_i is the relative humidity with respect to ice, and this time the temperatures are in the domain of the vapor-ice equilibrium curve. The equilibrium condition between ice and liquid results in

$$s_i(T) = s_l(T) - \frac{L_f(T)}{T} \quad (61)$$

Although, equations (59-61) are defined for different temperature ranges, they all include the triple point of water. Evaluation of those equations at the triple point shows that the reference constants in the entropy definition of the water phases are

not independent. Choosing the triple point of water as the reference point as before results in the following relationships among the constants:

$$s_{vr} = s_{lr} + \frac{L_v(T_r)}{T_r} \quad (62)$$

$$s_{vr} = s_{ir} + \frac{L_s(T_r)}{T_r} \quad (63)$$

$$s_{ir} = s_{lr} - \frac{L_f(T_r)}{T_r} \quad (64)$$

Only two of these equations are independent leaving one of the constants arbitrary. Once a value for one of the constants is selected, the other two are fixed by the above equilibrium requirements.

Since the entropy per unit mass of a system is simply the mass weighted average of the entropy of the subsystems

$$s = \sum_j q_j s_j \quad (65)$$

where s_j is given by equation (55) and the reference constants are constrained by equations (62–64), a general expression for the entropy per unit mass of the system can be written as

$$\begin{aligned} s = & \sum_j q_j c_{pj} \ln(T_j/T_r) \\ & + q_v \left[\frac{L_v(T_r)}{T_r} - R_v \ln(P_v/P_r) \right] - q_d R_d \ln(P_d/P_r) - (q_{ci} + q_{pi}) \frac{L_f(T_r)}{T_r} \end{aligned} \quad (66)$$

where the reference constants for dry air and liquid water have been set to zero. Since it is often handy to have an expression of entropy per unit of dry air mass, we note that because mass fractions are related to mixing ratios, $q_j = q_d r_j$, such expression is directly obtained dividing equation (66) by the mass fraction of dry air.

Our expression for the entropy of the system is very similar to that given in Hauf and Höller (1987). Our expression, as theirs, also neglects all effects associated with the configuration entropy of the droplet spectrum. There are, however, some differences: 1) In our expression, all water components do not have to have the same temperature. This is so because the entropy is an extensive quantity. Therefore, the total entropy is the sum of the entropies of the subsystems, which do not have to be in mutual thermal equilibrium. 2) In our derivation, the reference constants for the entropies of the water phases were chosen so the expressions for those entropies comply with the restrictions imposed on the system when it is brought into equilibrium. Although Hauf and Höller are aware of this, the constants given in their paper together with their equation (3.1) lead to a latent heat of vaporization of $1.858 \times 10^6 \text{ J kg}^{-1}$ and a latent heat of fusion of $21.917 \times 10^5 \text{ J kg}^{-1}$ at 273.15K in a saturated environment. This values are significantly different from the accepted figures for those latent heats.

In their paper, Hauf and Höller have pointed out the relation between the entropy and all potential temperatures used in atmospheric sciences. They show clearly that entropy provides a unified view for processes where some potential temperature is conserved.

References

Brown, R. G. and Zhang, C., 1997: Variability of midtropospheric moisture and its effect on cloud-top height distribution during TOGA COARE. *J. Atmos. Sci.*, **54**, 2760–2774.

de Groot, S. R. and Mazur, P., 1962: *Non-Equilibrium Thermodynamics*. North-Holland Publishing, 510.

Emanuel, K. A., 1994: *Atmospheric Convection*. Oxford University Press, 580.

Emanuel, K. A., Neelin, J. D., and Bretherton, C. S., 1994: On large-scale circulations in convecting atmospheres. *Quart. J. Roy. Meteorol. Soc.*, **120**, 1111–1143.

Flament, P. and Bernstein, R., 1993: . Images from the gms-4 satellite during toga-coare (november 1992 to february 1993). Technical report, School of Ocean and Earth Science and Technology, University of Hawaii, Honolulu. (20 pg, with two CD-ROMs).

Gray, W., 1973: Cumulus convection and larger scale circulations. part i: Broadscale and mesoscale considerations. *Mon. Weather Rev.*, **101**, 839–855.

Hauf, T. and Höller, H., 1987: Entropy and potential temperature. *J. Atmos. Sci.*, **44**, 2887–2901.

Houze, Jr., R. A., 1993: *Cloud Dynamics*. Academic Press, 573.

Johnson, R. H., Rickenbach, T. M., Rutledge, S. A., Ciesielski, P. E., and Schubert, W. H., 1999: Trimodal characteristics of tropical convection. *J. Climate*, **12**, 2397–2418.

Kingsmill, D. E. and Jr, R. A. H., 1999: Kinematic characteristics of air flowing into and out precipitation convection over the west pacific warm pool: An airborne doppler radar survey. *Quart. J. Roy. Meteorol. Soc.*, **125**, 1165–1270.

- Neelin, J. D. and Held, I. M., 1987: Modeling tropical convergence based on the moist static energy budget. *Mon. Weather Rev.*, **115**, 3–12.
- Raymond, D. J., 1995: Regulation of moist convection over the west Pacific warm pool. *J. Atmos. Sci.*, **15**, 3945–3959.
- Raymond, D. J., 2000: Thermodynamic control of tropical rainfall. *Quart. J. Roy. Meteorol. Soc.*, **126**, 889–898.
- Raymond, D. J., López-Carrillo, C., and Cavazos, L. L., 1998: Case studies of developing east Pacific easterly waves. *Quart. J. Roy. Meteorol. Soc.*, **124**, 2005–2034.
- Raymond, D. J. and Zeng, X., 2004: Modelling tropical atmospheric convection in the context of the weak temperature gradient approximation. *Quart. J. Roy. Meteorol. Soc.* In press.
- Sherwood, S. C., 1999: Convective precursors and predictability in the tropical western Pacific. *Mon. Weather Rev.*, **127**, 2977–2991.
- Tompkins, A. and Craig, G., 1998: Radiative-convective equilibrium in a three-dimensional cloud ensemble model. *Quart. J. Roy. Meteorol. Soc.*, **124**, 2073–2097.
- Webster, P. J. and Lukas, R., 1992: TOGA COARE : The coupled ocean-atmosphere response experiment. *Bull. Amer. Meteorol. Soc.*, **73**, 1377–1416.

Date (yyymmdd)	Sounding (UTC)	Aircraft (UTC)	Separation (km)
921126	<i>Shiyan 3</i> (-0115)	W43 (0338–0636)	250
921128	<i>Moana Wave</i> (0441)	W42 (0352–0445)	20
921212	Kapingamarangi (1706)	W42 & W43 (1747–1826)	665
921213	Kapingamarangi (1656)	W43 (1826–2041)	435
921215	<i>Xiangyanghong 5</i> (1714)	W42 (1713–1837)	160
930111	<i>Moana Wave</i> (2255)	W42 (2256–2520)	75
930116	<i>Shiyan 3</i> (2302)	W42 (2311–2430)	200
930118	<i>Shiyan 3</i> (2300)	W43 (0211–0355)	350
930201	<i>Moana Wave</i> (2257)	W42 (2251–2351)	70
930209	<i>Xiangyanghong 5</i> (1646)	W42 & W43 (1632–1841)	505

Table 1: Sounding and aircraft data sources used in section 4.2. The columns from left to right: (1) date; (2) sounding station(launching time) ; (3) aircraft(selected time interval); (4) average distance between sounding and aircraft target area.

Date	$\overline{\delta q_m}$	I_{NB}	$I_{NS} \times T_s$
(yymmdd)	(g kg ⁻¹)	(W m ⁻²)	(W m ⁻²)
921126	2.7942	+79.8 (?)	+51.3 (Moistening)
921128	3.0913	+196.7 (?)	+238.2 (Moistening)
921212	2.1534	-626.1 (Drying)	-710.1 (?)
921213	1.6041	-265.0 (Drying)	-288.9 (?)
921215	1.6704	-689.9 (Drying)	-782.7 (?)
930111	2.9783	+43.5 (?)	+58.5 (Moistening)
930116	2.3899	-4.1 (Drying)	-6.0 (?)
930118	2.5759	+8.2 (?)	+19.5 (Moistening)
930201	3.3477	+138.1 (?)	+156.6 (Moistening)
930209	2.3633	-405.6 (Drying)	-493.2 (?)

Table 2: Results from section (4.2). Columns left to right: (1) date of the aircraft mission; (2) average of the saturation deficit over a 9km-deep layer (1-10 km); (3) lateral contribution to the reduced energy tendency ; (4) lateral contribution to the reduce entropy tendency multiplied by a constant temperature, $T_s = 300$ K.

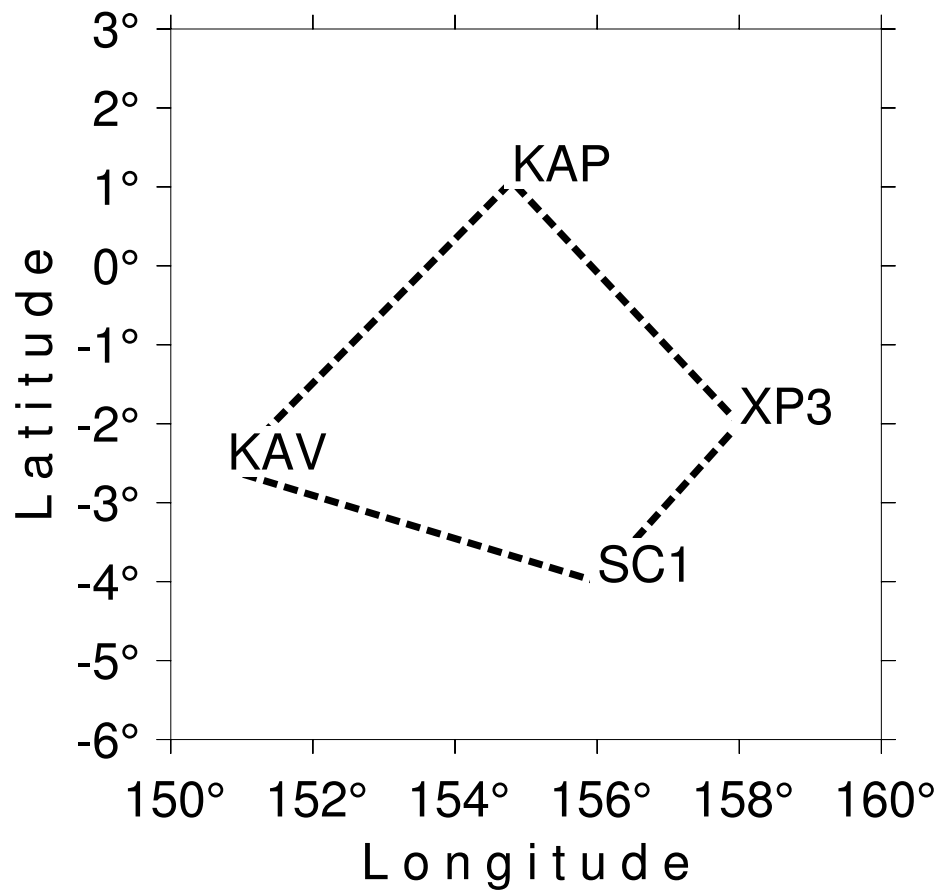


Figure 1: Area of the IFA (Intensive Flux Array) studied during the field phase of TOGA-COARE. The sounding launch sites at the corners of the IFA are the vessels *Shiyan 3* (SC1) and *Xiangyanghong 5* (XP3), and the islands of Kapingamarangi (KAP) and Kavieng (KAV).

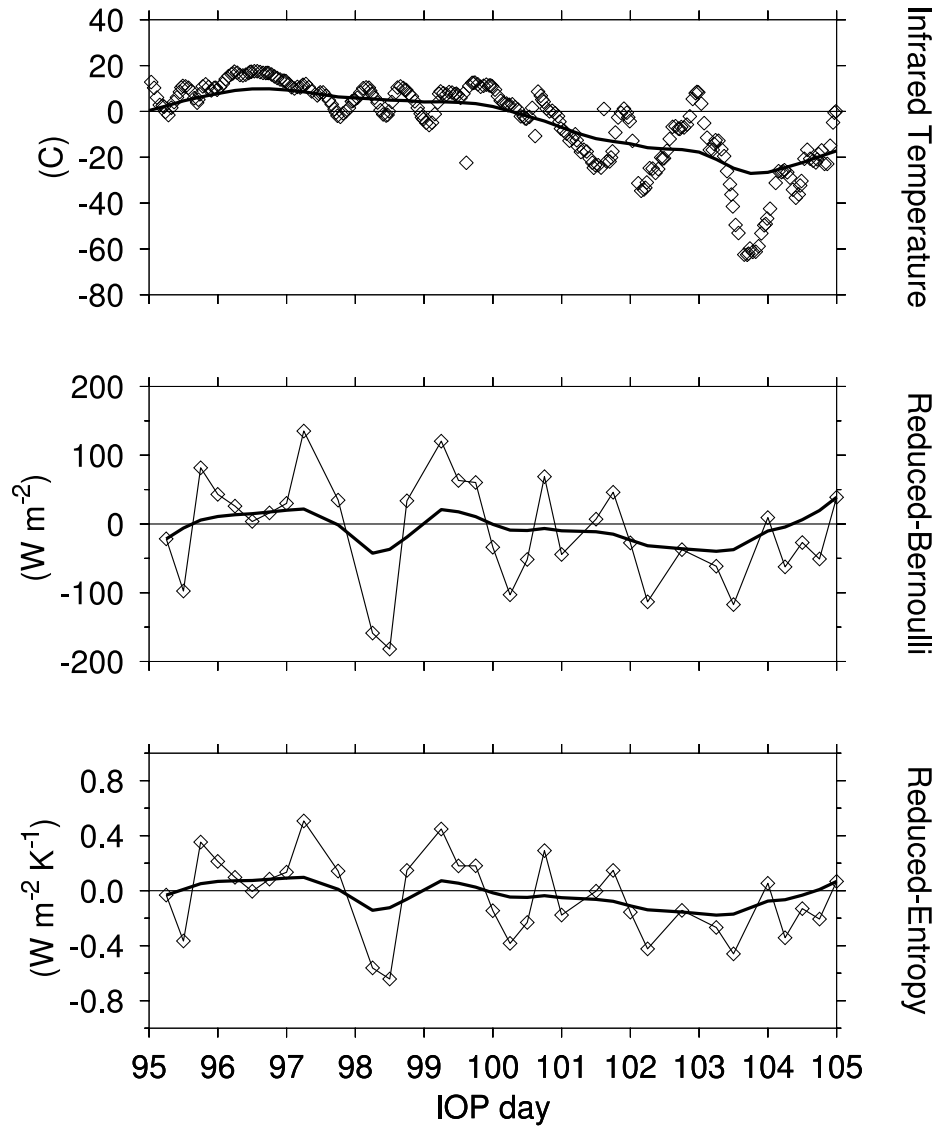


Figure 2: Upper panel shows the time series of the infrared satellite temperature averaged over the IFA region. The lateral import per unit volume of the reduced Bernoulli and entropy functions are shown in the middle and lower panels, respectively. For all panels, diamonds represent actual data and thick solid lines show the one-day smoothed version of the time series.

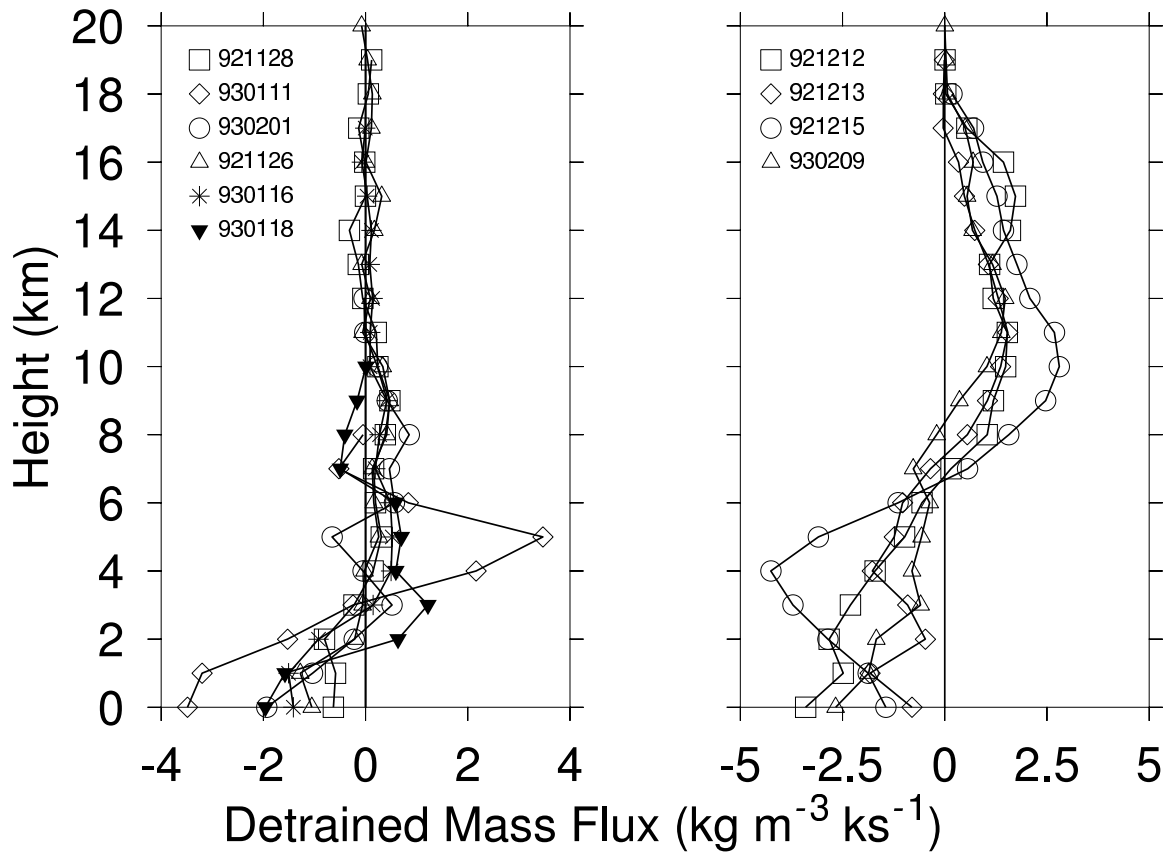


Figure 3: Detrained mass flux profiles for the ten case-studies examined here. They are grouped according to the depth of their inflow layer. The legends show the date (yymmdd) when the mission was flown.

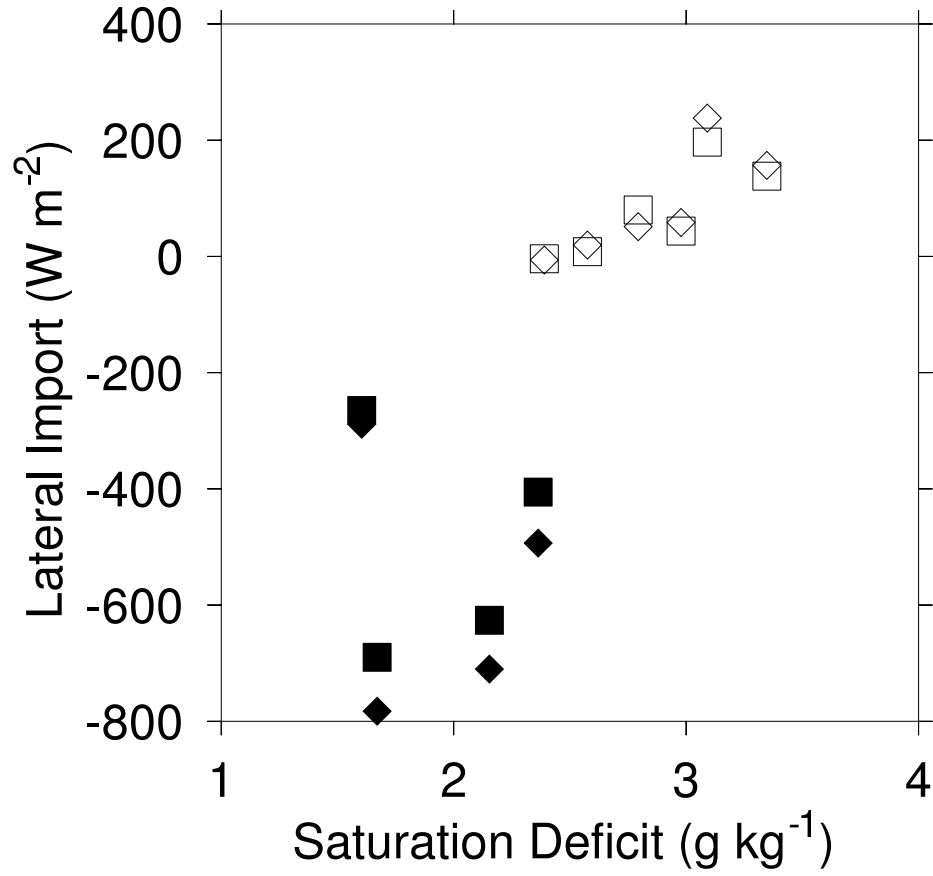


Figure 4: In this figure, squares represent the lateral import of the reduced Bernoulli function, while diamonds represent the import of reduced entropy multiplied by a constant temperature, $T_s = 300$ K. Filled symbols correspond to systems with deep inflow layers while non-filled symbols correspond to systems with shallow inflow layers – see figure 3 .